AIMS Materials Science, 4(4): 982-990.
DOI:10.3934/matersci.2017.4.982
Received: 14 June 2017
Accepted: 16 August 2017
Published: 01 September 2017

http://www.aimspress.com/journal/Materials

Research article

Structural, magnetic and electric properties of Nd and Ni co-doped $BiFeO_3$ materials

Dao Viet Thang [1,2,*], Le Thi Mai Oanh [2], Nguyen Cao Khang [2], Nguyen Manh Hung [1], Do Danh Bich [2], Du Thi Xuan Thao [1], and Nguyen Van Minh [2]

[1] Department of Physics, Hanoi University of Mining and Geology, Duc Thang Ward, North Tuliem District, Hanoi, Vietnam
[2] Center for Nano science and Technology, Physics Faculty, Hanoi National University of Education, 136 Xuan Thuy Road, Hanoi, Vietnam

*** Correspondence:** Email: daovietthang@humg.edu.vn; Tel: +84985811377.

Abstract: Multiferroic $Bi_{1-x}Nd_xFe_{0.975}Ni_{0.025}O_3$ (x = 0.00, 0.05, 0.10, 0.125, and 0.15) (BNFNO) and $BiFeO_3$ (BFO) materials were synthesized by a sol-gel method. Crystal structure, ferromagnetic and ferroelectric properties of the as-synthesized materials were investigated. Results showed that Nd^{3+} and Ni^{2+} co-doping affected to the electrical leakage, enhanced ferroelectric polarization and magnetization of $BiFeO_3$. Co-doped sample with 12.5 mol% of Nd^{3+} and 2.5 mol% of Ni^{2+} exhibited an enhancement in both ferromagnetism and ferroelectric properties up to M_S ~ 0.528 emu/g and P_S ~ 18.35 μC/cm^2 with applied electric field at 5 kV/cm, respectively. The origins of ferromagnetism and ferroelectricity enhancement were discussed in the paper.

Keywords: multiferroic; ferromagnetic; ferroelectric; polarization

1. Introduction

Due to the coexistence of ferroelectric, ferromagnetic and ferroelastic orders, multiferroic materials have been attracting extremely attention of many research groups. Multiferroics exhibited potential applications in fabrication of some electronic devices such as spintronics, multi-state memories, low-field ferromagnetic sensors, and actuators [1,2]. Among the very rare natural multiferroics, bismuth iron oxide $BiFeO_3$ (BFO), a rhombohedrally distorted perovskite, is ferroelectric below T_C ~ 1103 K and antiferromagnetic below T_N ~ 643 K [3,4]. The stereo-chemical

activity of Bi $6s^2$ lone-pair electrons is responsible for non-centrosymmetric ferroelectric order along <111> direction of the cubic perovskite-like lattice [5]. However, the appearance of impurities phases in pure BFO material leads to a high leakage current, a weak ferromagnetic order, and a wide range of transition temperature [4,6]. Therefore, pure BFO material does not well respond to practical applications. In order to solve these problems, a chemical modification of doping rare-earth or transition metal ions into Bi-sites or Fe-sites in BFO crystal lattice was strongly recommended [7,8]. Many works have reported the enhancement of magnetic property, in which Bi-sites were replaced by rare-earth (*RE*) ions (Ho^{3+}, La^{3+}, Nd^{3+}, Sm^{3+}) or Fe-sites were replaced by transition metal (*TM*) ions (Ni^{2+}, Co^{2+}) [9,10,11]. The magneto-electric (ME) effects on these materials were assigned to the coupling between ferroelectric order resulting from electron lone pair of Bi^{3+} ions and the ferromagnetic (or antiferromagnetic) order resulting from the doping ions [12]. Besides, the enhancement of magnetization in BFO was also attributed to the repression of cycloid spin structure. Raghavan et al. [13] and Li et al. [14] showed that *RE* and *TM* ions co-substitution was a promising route to improve multiferroic properties due to the reduction of leakage current and the enhancement of magnetization. This can be well explained because *RE* substitution for the Bi-sites was considered as an effective method to decrease leakage current and enhance the magnetization while *TM* substitution for the Fe-sites contributed to the improvement of ferroelectric property [15,16]. Therefore, *RE* and *TM* co-doping has been expected to enhance both ferroelectric and ferromagnetic properties [17,18].

In this paper, Nd and Ni co-doped BFO was synthesized by a sol-gel method in which Ni^{2+}-substituted concentration was kept at 2.5 mol% while Nd^{3+}-substituted concentration varied from 0 to 15 mol%. The influence of Nd^{3+} and Ni^{2+} co-doping as well as the influence of Nd concentration on microstructure, surface morphology, ferroelectric and ferromagnetic properties were investigated to find out the optimise Nd^{3+} concentration for the enhancement of multiferroic property in $BiFeO_3$ material.

2. Materials and Method

2.1. Materials

Iron nitrate ($Fe(NO_3)_3\ 9H_2O$), bismuth nitrate ($Bi(NO_3)_3\ 5H_2O$), neodymium nitrate ($Nd(NO_3)_3\ 6H_2O$), nickel(II) nitrate ($Ni(NO_3)_2\ 6H_2O$), ethylene glycol and citric acid were used for the preparation of BNFNO and BFO materials.

2.2. Preparation of Samples

BNFNO and BFO powders were synthesized by a sol-gel method. Firstly, $Fe(NO_3)_3\ 9H_2O$, $Bi(NO_3)_3\ 5H_2O$, and $Nd(NO_3)_3\ 6H_2O$ were mixed together in a correct weight proportion. The mole of $Fe(NO_3)_3\ 9H_2O$, $Bi(NO_3)_3\ 5H_2O$, and $Nd(NO_3)_3\ 6H_2O$ depended on x index (x = 0.00, 0.05, 0.10, 0.125, and 0.15). The mole ratio of these chemicals was 0.975, $(1 - x)$, and x, respectively. Afterwards, these chemicals were dissolved in 15 ml distilled water to get an aqueous solution. Then, this solution was stirred continuously at temperature 50–60 ℃ for an hour. Now, 35 ml solution of citric acid and ethylene glycol (with citric acid/ethylene glycol volume ratio 7/3) was added. After that, the last solution was evaporated at 100 ℃ for five hours to abtain wet gel. Finally, the wet gel

was heated at temperature 800 ℃ for seven hours to remove organic, and get BNFNO and BFO powders.

BNFNO samples with 2.5 mol% Ni^{2+}-substituted concentration and various Nd^{3+}-substituted concentration were labeled according to *x* index in the general chemical formula of $Bi_{1-x}Nd_xFe_{0.975}Ni_{0.025}O_3$ (x = 0.00, 0.05, 0.10, 0.125, and 0.15).

For the investigation of ferroelectric properties, the BNFNO and BFO powders were compressed into round tablets of 6 mm in diameter under the pressure of 20 MPa. Then, tablets were sintered at 800 ℃ for 5 hours to obtain ceramic samples. Next, two sides of the tablets were polished to achieve accurate thickness of 1 mm and high smoothness. After that, Pt electrodes were coated on both sides and then heated at 500 ℃ for three hours for a good contact between Pt electrodes and ceramic tablet.

2.3. Characterization

Crystal structure of BNFNO and BFO powders were characterized by different techniques. X-ray diffraction (XRD) patterns was carried out by a D5005 diffractometer using Cu-Kα radiation in 2 theta angle range of 20–65 ° at a step size of 0.02 °. Raman scattering measurements were performed in a back scattering configuration by Jobin Yvon T64000 triple spectrometer equipped with a cryogenic change-coupled device (CCD) array detector and operated using 514.5 nm exciting beam of Ar ion laser. Surface morphology of the BNFNO and BFO powders were explored by scanning electron microscopy (SEM). Vibrating sample magnetometer (7404_VSM) was used to measure the magnetization hysteresis (*M-H*) loops of the BNFNO and BFO powders. The polarization electric hysteresis (*P-E*) loops at room temperature of sintered ceramics were measured by a ferroelectric tester (Radiant, Precision LC_10V).

3. Results and Discussion

3.1. X-ray Diffraction

The XRD patterns of BNFNO and BFO powders are shown in Figure 1a. The XRD patterns of pure BFO sample are in good accord with the powder data of JCPDS Card No. 71-2494, revealing the presence of single-phase $BiFeO_3$ rhombohedral structure (R_{3C}). As clearly seen, no secondary phases are found in the XRD patterns of BFO sample. For Nd and Ni co-doped BFO samples, almost all peaks of the XRD shift toward higher 2θ values which reveal a change in lattice constants. From data of the XRD, lattice constants of BNFNO and BFO samples were calculated using UnitCell software and then graphed as a function of Nd^{3+} concentration in Figure 1b.

For BFO sample, the lattice constants were determined to be a = 5.585 ± 0.001 Å and c = 13.866 ± 0.002 Å. For Nd and Ni co-doped BFO samples, it is clear that both lattice constants *a* and *c* were reduced gradually with increasing the concentration of Nd^{3+}. This was because the radius of Nd^{3+} (1.109 Å) and Ni^{2+} (0.63 Å) ions are smaller than that of Bi^{3+} (1.17 Å) and Fe^{3+} (0.635 Å) ions, respectively. Therefore, the change of lattice constants indirectly reveals the substitution of Nd^{3+} and Ni^{2+} ions into $BiFeO_3$ crystal lattice.

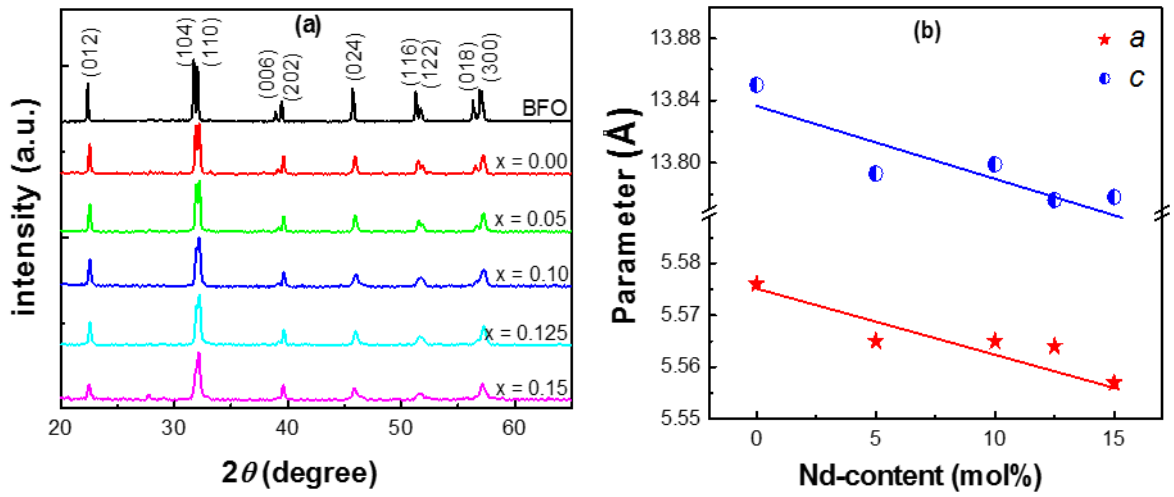

Figure 1. (a) X-ray diffraction patterns of BFO and $Bi_{1-x}Nd_xFe_{0.975}Ni_{0.025}O_3$ (x = 0.00, 0.05, 0.10, 0.125, and 0.15) powders; (b) the influence of lattice constants a and c as a function of the concentration of Nd^{3+}.

3.2. Raman Scattering Spectra

Raman scattering spectra of BNFNO and BFO powders measured at room temperature are shown in Figure 2. The previous studies have shown that Raman active modes of rhombohedral (R_{3C}) $BiFeO_3$ can be summarized in following irreducible representation: $\Gamma = 4A_1 + 9E$ [19,20]. In the wave number ranging from 100 to 400 cm^{-1}, Raman scattering spectra of BFO exhibited three A_1 modes at wave numbers of 132, 167, and 203 cm^{-1} and five E modes at wave numbers of 258, 275, 292, 318, and 355 cm^{-1}. Since Raman scattering spectra are very sensitive to atom displacements, the change in Raman peak position with increasing Nd^{3+} concentrations will indicate the substitution of Nd^{3+} for Bi^{3+} and the electrical polarization. The reason is that the stereo-chemical activity of the electron lone pair of Bi plays major role in the change of Bi–O covalent bonds, and characteristic modes observed at 132, 167, and 203 cm^{-1} for BFO sample. On the other hand, Gautam et al. [15] and Cazayous et al. [11] showed that these modes were supposedly believed to be responsible for the ferroelectric nature of the BFO sample. When Nd^{3+} concentration increases, there is a change in Bi–O covalent bonds as a result of the decline in the stereo-chemical activity of the electron lone pair of Bi and the long range ferroelectric order. The shift of Raman peaks towards higher wave numbers can be attributed to the change in the occupation states of Bi-site and the change in the Bi–O covalent bonds. If the vibration frequency is governed by local factors such as force constant and ion mass, it will be proportional to $(k/M)^{1/2}$ where k and M are force constant and ion mass, respectively. The shift of Raman peaks at high wave numbers, the reduction in intensity of prominent modes, and even the change in crystal structure are likely due to the lattice distortion at Bi-sites due to the substitution of Nd^{3+} ions which have lower atom weight (144.2 g) comparing to that of Bi atom (209.0 g). Furthermore, the electron lone pair of Bi effectively reduces the k-value that is inversely proportional to the length of Bi/Nd–O bond. Thus, the shift of Raman modes toward higher frequency shows an increase of k value and an decrease of Bi/Nd–O bond length. This result shows that Bi^{3+}-sites have been replaced by Nd^{3+} ions.

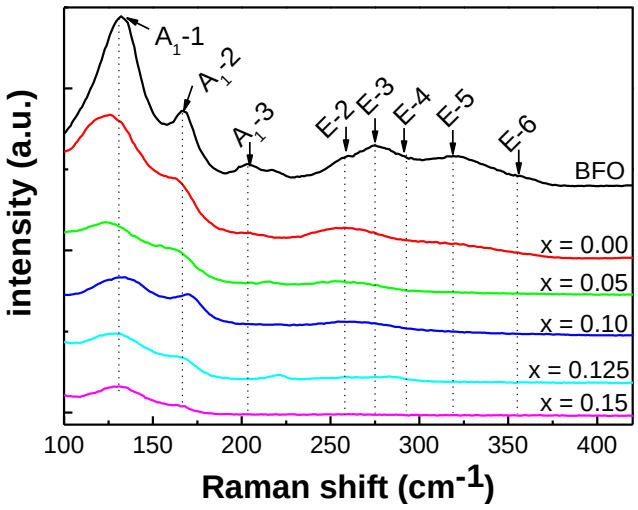

Figure 2. Raman scattering spectra of BFO and $Bi_{1-x}Nd_xFe_{0.975}Ni_{0.025}O_3$ (x = 0.00, 0.05, 0.10, 0.125, and 0.15) powders.

3.3. SEM Images

SEM images of BNFNO (x = 0.00, 0.05, 0.10, and 0.15) powders are in Figure 3. These images show that highly dense microstructure can be obtained by increasing Nd^{3+} concentration in BNFNO samples. The grains exhibit in-homogenous rectangular microstructures with different sizes and shapes. It is clear that the average grain size decreases with increasing of Nd^{3+} concentration. This is because the decrease of surface energy (or grain boundaries energy) caused by the interaction between the grains and surface leads to the stabilization of surfaces (or boundaries). Kumarn et al. [21] showed that the main reason of the decrease of grain size was because the bond dissociation energy of Gd–O bond was stronger than that of Bi–O bond.

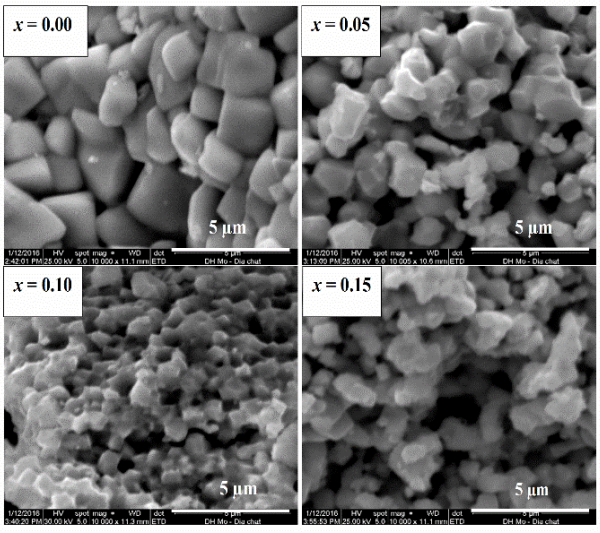

Figure 3. SEM images of $Bi_{1-x}Nd_xFe_{0.975}Ni_{0.025}O_3$ (x = 0.00, 0.05, 0.10, and 0.15) powders.

3.4. Ferromagnetic Properties

The magnetization hysteresis loops of as-synthesized powders were measured by VSM at room temperature with a maximum magnetic field of 10 kOe, as shown in Figure 4a. All samples show the indication of weak ferromagnetism. The saturation magnetization (*Ms*) and remnant magnetization (*Mr*) values of BNFNO samples are graphed in Figure 4b. *Ms* and *Mr* values increase when the concentration of Nd^{3+} increases from $x = 0.00$ to $x = 0.125$, and then decrease with further increasing of the concentration of Nd^{3+} to $x = 0.15$. The increase of magnetism can be explained by some causes: (i) the destruction of the antiferromagnetic order due to the substitution; (ii) the creation of oxygen vacancies as Ni replaced into Fe-sites; (iii) the modification of the spiral spin structure caused by the decrease of Fe–O–Fe bond angles associated with the distortion of crystal structure which is due to the difference in radius of ion Nd^{3+} and Bi^{3+}, leading to the decrease of Fe–O bond lengths and Fe–O–Fe bond angles as Nd^{3+} replaced into Bi^{3+}-sites [22]; (iv) the appearance of new magnetic interactions such as Nd^{3+}–Nd^{3+}, Nd^{3+}–Fe^{3+}, Nd^{3+}–Ni^{2+}, Fe^{3+}–Ni^{2+}, and Ni^{2+}–Ni^{2+} in addition to the regular exchange interaction of Fe^{3+}–Fe^{3+}. Kumarn et al. [21] reported that the weak ferromagnetism behavior in Gd-doped $BiFeO_3$ may be ascribed to partial destruction of spiral spin structure due to structural distortion and exchange interactions of Gd^{3+}–Gd^{3+} and Gd^{3+}–Fe^{3+}.

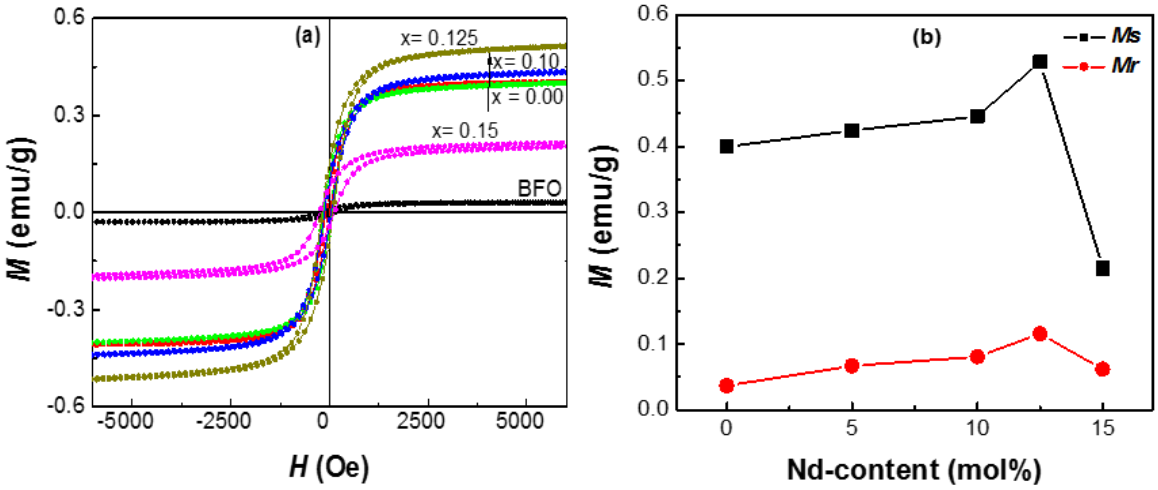

Figure 4. (a) Magnetization hysteresis loops of BFO and $Bi_{1-x}Nd_xFe_{0.975}Ni_{0.025}O_3$ (x = 0.00, 0.05, 0.10, 0.125, and 0.15) powders; (b) *Ms* and *Mr* values depend on concentration of Nd^{3+}.

3.5. Ferroelectric Properties

The ferroelectric (*P-E*) hysteresis loops of as-synthesized sintered ceramics are shown in Figure 5a. The shape of *P-E* loops indicates that all samples exhibit ferroelectric behavior. When the concentration of Nd^{3+} increases, the shape of the *P-E* loops changed distinctively which reveals that Nd and Ni co-doping is effective in increasing the ferroelectric behavior of BFO. The increasing of Nd^{3+} concentration causes an increase in dielectric constant and decrease in leakage current as shown in Figure 5b. The main reasons can be assigned to the presence of oxygen vacancies, resulting to

virtual hopping of electrons between Fe^{2+} and Fe^{3+}. Rajput et al. [23] also demonstrated the increase of ferroelectric polarization as co-doping La and Ni into BFO materials. The enhanced ferroelectric properties of samples were attributed to the reduction of leakage current. Remnant polarization (*Pr*) and saturation polarization (*Ps*) increase gradually with doping concentration in which *Pr* values are 0.15, 2.80, 2.85, 3.39, and 9.97 μC/cm^2 and *Ps* values are 0.33, 4.16, 7.07, 7.49, and 18.35 μC/cm^2 for BNFNO (x = 0.00, 0.05, 0.10, 0.125, and 0.15) samples, respectively.

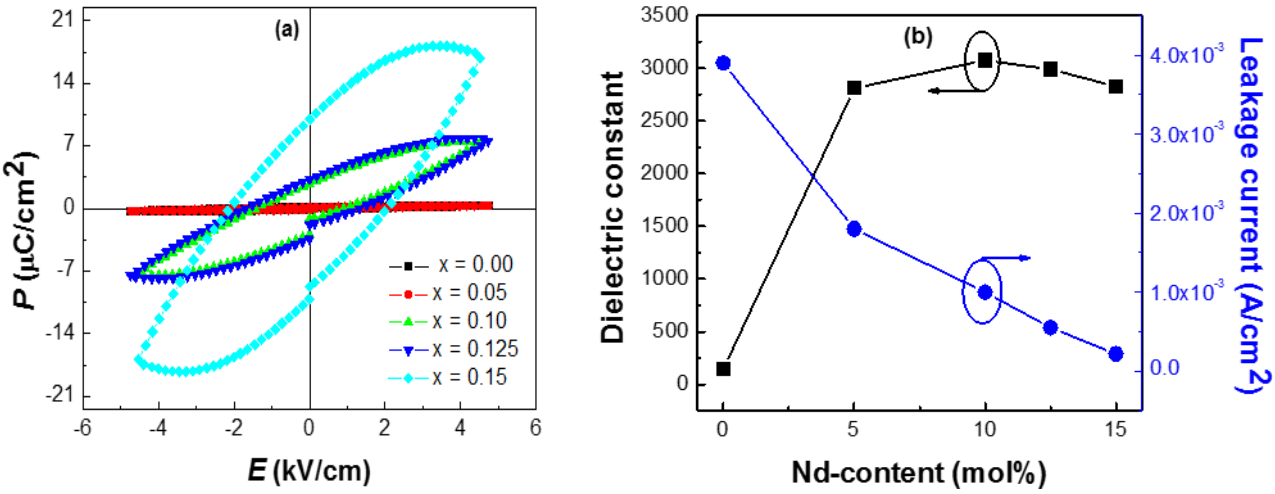

Figure 5. (a) Polarization electric hysteresis loops; (b) dielectric constant and leakage current of $Bi_{1-x}Nd_xFe_{0.975}Ni_{0.025}O_3$ (x = 0.00, 0.05, 0.10, 0.125, and 0.15) sintered ceramics.

4. Conclusion

In summary, the effects of Nd and Ni co-doping on the microstructure, ferroelectric and ferromagnetic properties of BFO have been investigated. The results showed the improvement of both ferroelectric and ferromagnetic properties when co-doping Nd and Ni into $BiFeO_3$. The saturation ferroelectric polarization and remnant polarization increased from *Ps* = 0.33 μC/cm^2 and *Pr* = 0.15 μC/cm^2 for BNFNO with x = 0.00 up to P_S = 18.35 μC/cm^2 and *Pr* = 9.97 μC/cm^2 for BNFNO with x = 0.015. The saturation magnetization *Ms* also increased from 0.40 emu/g for BNFNO with x = 0.00 up to 0.528 emu/g for BNFNO with x = 0.125. These results suggested that Nd and Ni co-doped BFO materials can be used for applications in multiferroic memory devices.

Acknowledgments

The authors thanks for the help of Hanoi University of Mining and Geology.

Conflict of Interest

The authors declare that there is no conflict of interest.

References

1. Eerenstein W, Mathur ND, Scott JF (2006) Multiferroic and magnetoelectric materials. *Nature* 442: 759–765.
2. Tokura Y (2007) Multiferroics-toward strong coupling between magnetization and polarization in a solid. *J Magn Magn Mater* 310: 1145–1150.
3. Qi X, Dho J, Tomov R, et al. (2005) Greatly reduced leakage current and conduction mechanism in aliovalention-doped $BiFeO_3$. *Appl Phys Lett* 86: 062903.
4. Kubel F, Schmid H (1990) Structure of a ferroelectric and ferroelastic monodomain crystal of the perovskite $BiFeO_3$. *Acta Crystallogr B* 46: 698–702.
5. Xi XJ, Wang SY, Liu WF, et al. (2014) Enhanced magnetic and conductive properties of Ba and Co co-doped $BiFeO_3$ ceramics. *J Magn Magn Mater* 355: 259–264.
6. Ruette B, Zvyagin S, Pyatakov AP, et al. (2004) Magnetic-field-induced phase transition in $BiFeO_3$ observed by high-field electron spin resonance: Cycloidal to homogeneous spin order. *Phys Rev B* 69: 064114.
7. Chakrabarti K, Das K, Sarkar B, et al. (2011) Magnetic and dielectric properties of Eu-doped $BiFeO_3$ nanoparticles by acetic acid-assisted sol-gel method. *J Appl Phys* 110: 103905.
8. Lazenka VV, Ravinski AF, Makoed II, et al. (2012) Weak ferromagnetism in La-doped $BiFeO_3$ multiferroic thin films. *J Appl Phys* 111: 123916.
9. Rao TD, Karthik T, Srinivas A, et al. (2012) Study of Structural, Magnetic and Electrical properties on Ho-substituted $BiFeO_3$. *Solid State Commun* 152: 2071–2077.
10. Xu X, Guoqiang T, Huijun R, et al. (2013) Structural, electric and multiferroic properties of Sm-doped $BiFeO_3$ thin films prepared by the sol-gel process. *Ceram Int* 39: 6223–6228.
11. Cazayous M, Malka D, Lebeugle D, et al. (2007) Electric field effect on $BiFeO_3$ single crystal investigated by Raman spectroscopy. *Appl Phys Lett* 91: 071910.
12. Chakrabarti K, Das K, Sarkar B, et al. (2012) Enhanced magnetic and dielectric properties of Eu and Co co-doped $BiFeO_3$ nanoparticles. *Appl Phys Lett* 101: 042401.
13. Raghavan CM, Kim JW, Kim SS (2013) Structural and ferroelectric properties of chemical solution deposited (Nd, Cu) co-doped $BiFeO_3$ thin film. *Ceram Int* 39: 3563–3568.
14. Li Y, Zhang H, Li Q, et al. (2012) Structural distortion and room-temperature ferromagnetization of Co-doped and (Eu, Co)-codoped $BiFeO_3$ nanoparticles. *Mater Lett* 87: 117–120.
15. Gautam A, Singh K, Sen K, et al. (2011) Crystal structure and magnetic property of Nd doped $BiFeO_3$ nanocrytallites. *Mater Lett* 65: 591–594.
16. Reddy VA, Pathak NP, Nath R (2013) Enhanced magnetoelectric coupling in transition-metal-doped $BiFeO_3$ thin film. *Solid State Commun* 171: 40–45.
17. Ye W, Tann G, Dong G, et al. (2015) Improved multiferroic properties in (Ho, Mn) co-doped $BiFeO_3$ thin films prepared by chemical solution deposition. *Ceram Int* 41: 4668–4674.
18. Coondoo I, Panwar N, Rafiq MA, et al. (2014) Structural, dielectric and impedance spectroscopy studies in $(Bi_{0.90}R_{0.10})Fe_{0.95}Sc_{0.05}O_3$ (R = La, Nd) ceramics. *Ceram Int* 40: 9895–9902.
19. Fukumura H, Harima H, Kisoda K, et al. (2007) Raman scattering study of multiferroic $BiFeO_3$ single crystal. *J Magn Magn Mater* 310: 367–369.
20. Singh MK, Jang HM, Ryu S, et al. (2006) Polarized Raman scattering of multiferroic $BiFeO_3$ epitaxial films with rhombohedral R3c symmetry. *Appl Phys Lett* 88: 042907.

21. Kumarn M, Sati PC, Chhoker S, et al. (2015) Electron spin resonance studies and improved magnetic properties of Gd substituted $BiFeO_3$ ceramics. *Ceram Int* 41: 777–786.
22. Suresh P, Srinath S (2014) Study of structure and magnetic properties of rare earth doped $BiFeO_3$. *Physica B* 448: 281–284.
23. Rajput SS, Katoch R, Sahoo KK, et al. (2015) Enhanced electrical insulation and ferroelectricity in La and Ni co-doped $BiFeO_3$ thin film. *J Alloy Compd* 621: 339–344.

AIMS Press